CAMS Service Evolution

D1.4 Report on aligning aerosol parameter retrievals

Due date of deliverable	Dec 2023
Submission date	Jan 2024
File Name	CAMEO-D1-4
Work Package /Task	Global aerosol assimilation in CAMS/ T1.2 Adaptation of aerosol parameter retrievals from 3MI, MAP/CO2M, S-3, -4,-5P and other instruments for the aerosol representation in CAMS (global)
Organisation Responsible of Deliverable	LOA, GRASP-SAS
Author name(s)	Pavel Litvinov, Oleg Dubovik, Cheng Chen, Milagros Herrera, Christian Matar, Marcos Herreras, Anton Lopatin
Revision number	1.0
Status	Issued
Dissemination Level	Public

Funded by the European Union

The CAMEO project (grant agreement No 101082125) is funded by the European Union.

1 Executive Summary

Aerosol modelling plays a crucial role in climate studies and air quality monitoring. Currently, significant differences exist between aerosol modelling methodologies employed in various remote sensing algorithms and global climate models. This divergence poses challenges in integrating remote sensing retrieval results into reanalysis efforts aimed at establishing climatological aerosol models for global climate models and forecasts.

This gap also impacts remote sensing approaches, as global climate models provide global information about aerosol masses emissions, accounting for atmospheric states, aerosol sources, and sinks. Consequently, the aerosol information predicted or derived climatologically from global climate models, such as aerosol type and vertical profile, serves as valuable a priori information to constrain remote sensing measurements.

Directly applying the CAMS aerosol modelling approach to remote sensing introduces complexities in the forward model and significantly increases the number of retrieved parameters. However, achieving harmonization between aerosol approaches in global climate modelling and remote sensing holds the potential to enhance the accuracy of aerosol retrieval, as well as climate monitoring and forecasting.

Table of Contents

2 Introduction

2.1 Background

Monitoring the composition of the atmosphere is a key objective of the European Union's flagship Space programme Copernicus, with the Copernicus Atmosphere Monitoring Service (CAMS) providing free and continuous data and information on atmospheric composition.

At present time there is a big gap between aerosol optics modelling approaches used in various remote sensing algorithms and in the global climate models such as CAMS. This complicates the implementation of the remote sensing retrieval results in the reanalysis for deriving climatological aerosol optical models for global climate models and forecasts.

This gap also has an effect on remote sensing approaches in reverse. In particular, the aerosol optics models used in the global climate models include a sophisticated scheme of global aerosol distribution taking into account atmospheric states, aerosol sources, its vertical distribution and sinks. Thus, the predicted or climatological aerosol information from global climate models (like predicted aerosol type, vertical profile, etc.) could be a valuable source of a priori information to constrain the retrieval of remote sensing measurements.

On the other hand, direct implementation of CAMS aerosol modelling approach to remote sensing may essentially complicate the forward modelling and considerably increase the number of retrieved parameters slowing down and destabilising the retrievals. At the same time, harmonization of the aerosol approaches between CAMS model and remote sensing may greatly enhance the accuracy of aerosol retrieval as well as climate monitoring and forecasting.

2.2 Scope of this deliverable

2.2.1 Objectives of this deliverables

This document provides the results of the feasibility studies on harmonization of aerosol optics modelling between GRASP retrieval algorithm and CAMS aerosol model.

2.2.2 Work performed in this deliverable

The harmonization of aerosol optics modelling between GRASP retrieval algorithm and CAMS aerosol model is the subject of the deliverable. For the task fulfilment, the following studies, tests and validations were performed:

1. Review of CAMS aerosol models and its adaptation for remote sensing retrieval algorithms.

2. Implementation of the CAMS aerosol optical model into the GRASP forward model.

3. Studies on the sensitivity of remote sensing retrieval to the parameters of the aerosol model and atmosphere state from the CAMS model.

4. Adaptation of CAMS aerosol optical model for the retrieval of remote sensing measurements.

Creation of CAMS-based aerosol optical model for remote sensing applications.

5. Harmonization of CAMS aerosol model obtained from reanalysis with CAMS-based aerosol model adapted for remote sensing applications.

6. Implementation of the adapted CAMS-based aerosol model for GRASP retrieval of remote sensing measurements.

7. MAP (3MI, S7 MAP, PARASOL) synthetic measurements simulation with GRASP using CAMS model.

8. Testing and validation of an adapted CAMS-based aerosol model on the synthetic measurements as well as on the real PARASOL and AERONET measurements using GRASP algorithm.

2.2.3 Deviations and counter measures

No deviations have been encountered.

2.2.4 CAMEO Project Partners:

ECMWF	EUROPEAN CENTRE FOR MEDIUM-RANGE WEATHER FORECASTS
Met Norway	METEOROLOGISK INSTITUTT
BSC	BARCELONA SUPERCOMPUTING CENTER-CENTRO NACIONAL DE SUPERCOMPUTACION
KNMI	KONINKLIJK NEDERLANDS METEOROLOGISCH INSTITUUT-KNMi
SMHI	SVERIGES METEOROLOGISKA OCH HYDROLOGISKA INSTITUT
BIRA-IASB	INSTITUT ROYAL D'AERONOMIE SPATIALEDE BELGIQUE
HYGEOS	HYGEOS SARL
FMI	ILMATIETEEN LAITOS
DLR	DEUTSCHES ZENTRUM FUR LUFT - UND RAUMFAHRT EV
ARMINES	ASSOCIATION POUR LA RECHERCHE ET LE DEVELOPPEMENT DES METHODES ET PROCESSUS INDUSTRIELS
CNRS	CENTRE NATIONAL DE LA RECHERCHE SCIENTIFIQUE CNRS
GRASP-SAS	GENERALIZED RETRIEVAL OF ATMOSPHERE AND SURFACE PROPERTIES EN ABREGE GRASP
CU	UNIVERZITA KARLOVA
CEA	COMMISSARIAT A L ENERGIE ATOMIQUE ET AUX ENERGIES ALTERNATIVES
MF	METEO-FRANCE
TNO	NEDERLANDSE ORGANISATIE VOOR TOEGEPAST NATUURWETENSCHAPPELIJK ONDERZOEK TNO
INERIS	INSTITUT NATIONAL DE L ENVIRONNEMENT INDUSTRIEL ET DES RISQUES - INERIS
IOS-PIB	INSTYTUT OCHRONY SRODOWISKA - PANSTWOWY INSTYTUT BADAWCZY
FZJ	FORSCHUNGSZENTRUM JULICH GMBH
AU	AARHUS UNIVERSITET
ENEA	AGENZIA NAZIONALE PER LE NUOVE TECNOLOGIE, L'ENERGIA E LO SVILUPPO ECONOMICO SOSTENIBILE

3 Aerosol models in the global transport models and remote sensing

3.1 Aerosol models in CAMS and MERRA-2 global transport models

CAMS (Copernicus Atmosphere Monitoring Service) combines observations with data assimilation and forecasting systems (Bozzo et al. 2020; Fleming et al. 2015, 2017, Rémy et al., 2022). Depending on the IFS (Integrated Forecasting System) cycles, the aerosol forward model used in CAMS can include 5-8 types of tropospheric aerosol species: sea salt (SS), dust (DU), hydrophilic and hydrophobic organic matter (OM), black carbon (BC), sulfate (SU), nitrate, ammonium, and secondary organics (SOA) aerosols. Each type consists of a few more components (aerosol tracer) with different microphysical and hygroscopic properties. The hygroscopic effects are taken into account for sulfates, sea salt, organic matter, nitrate, ammonium, and secondary organics (SOA) species. In total, the CAMS system operates with 11-15 aerosol trac tracer (components). It takes into account the dust emission depending on the surface wind, soil moisture and albedo. Emissions for sea salt depend on a source function based on Monahan et al. (1986). Emissions of OM, BC and SO2 linked to fire emissions are obtained using the Global Fire Assimilation System (GFAS) based on MODIS satellite observations of fire radiative power (Kaiser et al., 2011). The OM species include a contribution from organic carbon from biofuel, fossil fuel and biomass burning, with a small contribution of secondary organic aerosols from biogenic sources. Together, with pressure and humidity profiles and vertical profiles of aerosol mass mixing ratios for each aerosol component, CAMS provides detailed vertical characterization of different aerosol species.

3.1.1 Aerosol species

Here we analyse 5 aerosol species which are common in different CAMS IFS cycles and MERRA-2/GOCART model (Chin et al., 2002; Randles et al., 2017). Different aerosol species and their bins from CAMS and MERRA-2 are presented in Table 3.1.1.

Table 3.1.1. 5 aerosol species in CAMS and MERRA-2 optical models

	Aerosol		CAMS	MERRA-2 Natural Run
1	**BC**	Hydrophobic	X	X
		Hydrophilic	X	X
2	**OM**	Hydrophobic	X	X
		Hydrophilic	X	X
3	**SU Hydrophilic**		X	X
4	**Sea Salt**	SeaSalt1	X	X
		SeaSalt2	X	X
		SeaSalt3	X	X

	Aerosol		CAMS	MERRA-2 Natural Run
		SeaSalt4	-	X
		SeaSalt5	-	X
5	**Dust**	Dust1	X	X
		Dust2	X	X
		Dust3	X	X
		Dust4	Present in IFS 48R1 cycle	X
		Dust5	-	X

3.1.2 Size distribution

Size distribution and the complex refractive indices for BC, OM, and SU aerosol species are defined in a very similar way both in CAMS and MERRA-2 models. At the same time, the dust and sea salt size distributions assumed when computing offline the aerosol optical parameters are defined differently. In particular, the number of bins is different (Table 3.1). Up to the cycle 47R3, 3 dust bins in CAMS are defined within the range of the monomodal lognormal size distribution (Fig. 3.1.1).

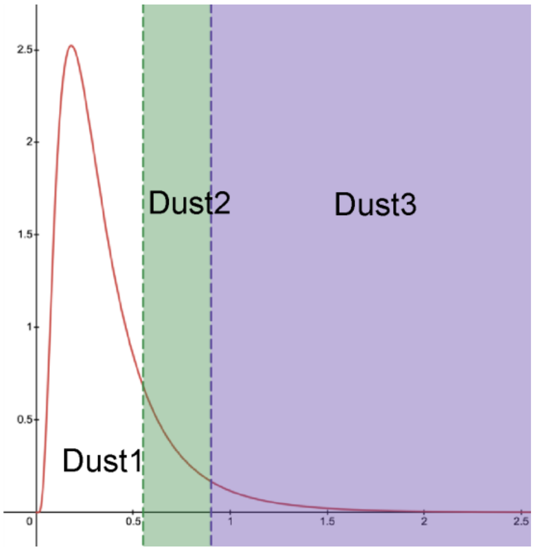

Figure 3.1.1: Dust bins from CAMS (OC and up to cycle 47R3).

3.1.2 Hygroscopicity

The CAMS aerosol optical model has the following dependence of the complex refractive index of all hydrophilic aerosol tracers on relative humidity (RH) as following:

$$\widehat{m}_{wet} = \widehat{m}_{dry}\delta_v + \widehat{m}_{water}(1 - \delta_v), \qquad (3.1.1)$$

where δ_v is volume fraction of dry aerosol:

$$\delta_v = \frac{V_{dry}}{V_{wet}} = \frac{1}{\left(f_{grow}\right)^3} \qquad (3.1.2)$$

The size of particles changes according to the tabulated value f_{grow} for each hydrophilic tracer (aerosol component).

3.1.3 Vertical profiling

The aerosol vertical profiles for each tracer (bin) in the CAMS aerosol optical model is represented by mass mixing ratio (MMR) defined at each vertical pressure level of the atmosphere. MMR can be related to volume ($c_v^{(k)}(z)$) or number ($n^{(k)}(z)$) aerosol concentration as following:

$$n^{(k)}(z) = M_{mix}^{(k)}(z)\frac{\rho_{air}(z)}{m_{dry}^{(k)}}, \qquad (3.1.3)$$

$$c_v^{(k)}(z) = \left(M_{mix}^{(k)}(z)\,\rho_{air}(z)\right)\frac{\left[f_{grow}^{(k)}(z)\right]^3}{\rho_{dry}^{(k)}}, \qquad (3.1.4)$$

where $M_{mix}^{(k)}(z)$ is aerosol mass mixing ratio, $\rho_{air}(z)$ is air density, $f_{grow}^{(k)}(z)$ aerosol size growth factor, $m_{dry}^{(k)}$ and $\rho_{dry}^{(k)}$ are dry aerosol mass and density at each atmospheric level k.

3.2 Aerosol models in remote sensing: GRASP algorithm

Aerosol optical models used in the remote sensing retrieval algorithm are usually much simpler in comparison to aerosol models in CAMS. Moreover, they vary between different retrieval algorithms and the most optimal one should correspond to information content of the measurements. In other words, the most optimal model for such full information content instruments like PARASOL/POLDER, 3MI or CO2M may be not optimal for the instruments with limited information content like S3/OLCI, MODIS, S5p/TROPOMI etc. Here to consider possible harmonization between aerosol optical models in remote sensing and global transport modelling we use as an example GRASP chemical component model, considered as the most optimal one for GRASP/PARASOL and future 3MI, CO2M MAP retrieval.

3.2.1 Aerosol components (modes)

GRASP/Components (Li et al., 2019) approach enables to add an extra layer of information by not retrieving directly the aerosol refractive index (real and imaginary parts), but to retrieve the concentration (in percent) corresponding to some preselected chemical species whose refractive index is prescribed. Thus, GRASP/Components approach is fully compatible with any other possible representation of aerosol microphysical properties, because it is only related with the refractive index representation. Furthermore, the spectral look-up-tables representing the different chemical components are designed in a generalized and flexible manner that enables to easily modify which species are taken into account in each application.

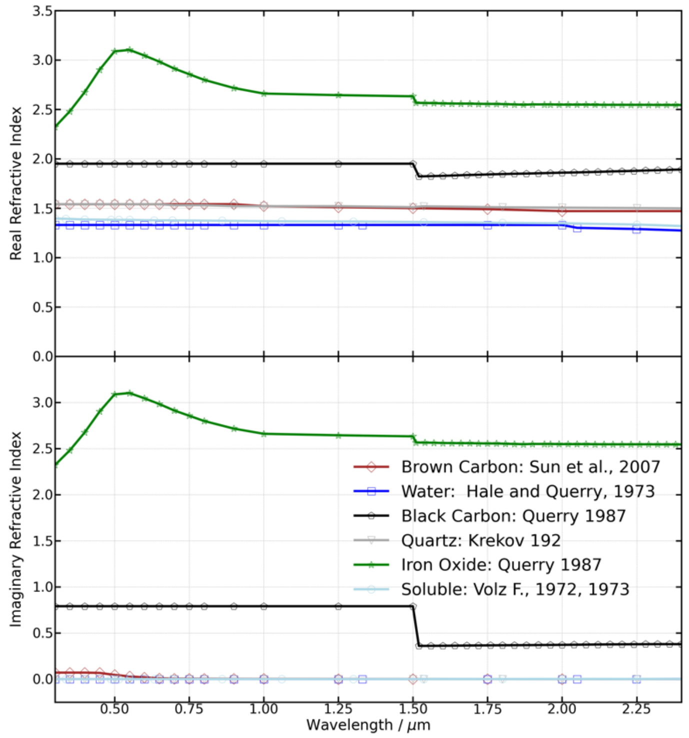

-

Figure 3.2.1: Spectral refractive index (real part in top panel, imaginary pat in bottom panel) of the aerosol chemical species assumed in GRASP/Components approach.

The refractive index of the standard components which are part of the aerosol optical model in GRASP/Components scheme is represented in Fig. 3.2.1. The chemical components in GRASP/Components approach are different for fine and coarse aerosol modes (Table 3.2.1):

- Fine mode: Black Carbon, Brown Carbon, Quartz and soluble species
- Coarse mode: Iron Oxide, Quartz and soluble species

Table 3.2.1. GRASP 2 aerosol modes and chemical components

	Size distribution	**Volume Concentration**	**BC**	**BrC**	**Quarts**	**Iron Oxide**	**Water/ Sulphate**
Fine mode	3 LN bins	✓	✓	✓	✓	X	✓
Coarse mode	2 LN bins	✓	X	X	✓	✓	✓

The refractive index of each of these chemical species is based on literature review and provided in the Section 3.2.1 and 3.3.1. Despite that there are some discrepancies between different authors to characterize this optical magnitude, here a selection of the most accepted references by the scientific community has been selected. This components selection is validated by a number of applications including satellite retrievals as POLDER or ground-based instruments as AERONET sunphotometers (Li et al., 2019, 2022; Zhang et al., 2021, 2022). Some examples, of the validation of the derived optical properties (such as AOD, SSA, and AE) are presented in Figs. 4.1.1 and 4.1.2.

3.2.2. Size distribution

Size distribution in fine mode is represented by 3 first bins, and coarse mode is described by two last bins (Fig.3.2.2).

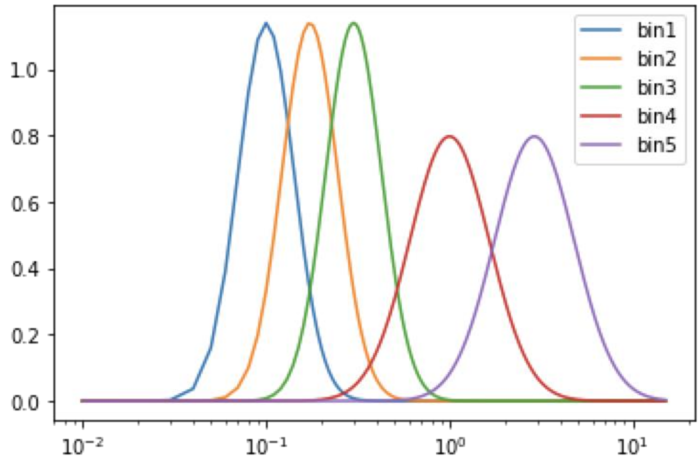

Figure 3.2.2: Size distribution of 5 log-normal bins in GRASP retrievals

The predefined parameters of the size distribution bins are presented in Table 3.3.3.

Table 3.2.2: Predefined parameters of 5 log-normal bins

Aerosol parameter	Value	Units	Description
$r_{V,1}$	0.100	μm	modal radius of volume SD, bin 1
$r_{V,2}$	0.1732	μm	modal radius of volume SD, bin 2
$r_{V,3}$	0.300	μm	modal radius of volume SD, bin 3
$r_{V,4}$	1.000	μm	modal radius of volume SD, bin 4
$r_{V,5}$	2.900	μm	modal radius of volume SD, bin 5
σ_1	0.350	-	logarithm of dispersion of volume SD, bin 1
σ_2	0.350	-	logarithm of dispersion of volume SD, bin 2
σ_3	0.350	-	logarithm of dispersion of volume SD, bin 3
σ_4	0.500	-	logarithm of dispersion of volume SD, bin 4
σ_5	0.500	-	logarithm of dispersion of volume SD, bin 5

3.2.3 Vertical profiling

In most remote sensing retrieval algorithms, such optical properties of aerosol as the phase matrix, cross sections and Single Scattering Albedo (SSA) for each aerosol component k (or mode) are usually considered to be the same in all atmospheric layers (column averaged phase matrix $< P_k >$, scattering and extinction cross sections ($< C_{v\,sc}^{(k)} >$ and $< C_{v\,ext}^{(k)} >$), SSA ($< \omega^{(k)} >$)):

$$< P_k >= \frac{\int_{z_1}^{z_{lmax}} P_k(z')C_{v\,sc}^{(k)}(z')c_v^{(k)}(z')dz'}{\int_{z_1}^{z_{lmax}} C_{v\,sc}^{(k)}(z')c_v^{(k)}(z')dz'} \qquad (3.2.1)$$

$$< C_{v\,sc}^{(k)} >= \frac{\int_{z_1}^{z_{lmax}} C_{v\,sc}^{(k)}(z')c_v^{(k)}(z')dz'}{\int_{z_1}^{z_{lmax}} c_v^{(k)}(z')dz'}, \qquad (3.2.2)$$

$$< C_{v\,ext}^{(k)} >= \frac{\int_{z_1}^{z_{lmax}} C_{v\,ext}^{(k)}(z')c_v^{(k)}(z')dz'}{\int_{z_1}^{z_{lmax}} c_v^{(k)}(z')dz'}. \qquad (3.2.3)$$

$$< \omega^{(k)} >= \frac{< C_{v\,sc}^{(k)} >}{< C_{v\,ext}^{(k)} >} \qquad (3.2.4)$$

The vertical distribution of aerosol in atmosphere is accounted with aerosol concentration (number $n^{(k)}(z)$ or volume $c_v^{(k)}(z)$ concentration) or extinction profile $< \alpha_l^{(k)}(z) >$ which can be different for different aerosol component *k* (modes):

$$< \alpha_l^{(k)}(z) > = < C_{v\,ext}^{(k)} > c_v^{(k)}(z). \qquad (3.2.5)$$

Very often, the concentration profiles in remote sensing retrieval algorithms is approximated by simplified vertical distributions, for example, by the exponential one:

$$c_v^{(k)}(z) = c_{0v}^{(k)} \frac{1}{h} exp\; exp\; \left(-\frac{z}{h}\right), \qquad (3.26)$$

$$n^{(k)}(z) = n_0^{(k)} \frac{1}{h} exp\; exp\; \left(-\frac{z}{h}\right), \qquad (3.27)$$

where $c_{0v}^{(k)}$ is total column volume and $n_0^{(k)}$ number concentration for aerosol component *k*.

3.2.4 Internal mixture of chemical components

The complex refractive index for internal mixture in GRASP can be calculated using Maxwell-Garnett or linear volume mixture approaches. Both approaches show quite similar performance on real PARASOL measurement (Section 4.1, Figs. 4.1.1 and 4.1.2). In the representation given in Table 3.2.1 and in the case of linear volume mixture approach it can be calculated for fine and coarse modes as following:

$$\widehat{m}_{eff}^{fine} = \widehat{m}_{BC}\delta_{BC} + \widehat{m}_{BrC}\delta_{BrC} + \delta_{Quartz}^{fine} + \left(1 - \delta_{BC} - \delta_{BrC} - \delta_{Quartz}^{fine}\right)\widehat{m}_{Solub}, \qquad (3.28)$$

$$\widehat{m}_{eff}^{coarse} = \widehat{m}_{Quartz}\delta_{Quartz}^{coarse} + \widehat{m}_{Iron}\delta_{FeOx} + \left(1 - \delta_{Quartz} - \delta_{FeOx}\right)\widehat{m}_{Solub}, \qquad (3.29)$$

where δ denotes the volume fraction of each chemical component correspondingly.

3.3 GRASP aerosol components and CAMS species

3.3.1 Refractive index

Intercomparison of the refractive indices used in these studies of CAMS (from IFS cycles 47R1 and 48R1) and MERRA-2 aerosol species and GRASP baseline chemical component is presented in Figs. 3.3.1-3.3.5. Table 3.3.1 contains the literature references for the refractive indices.

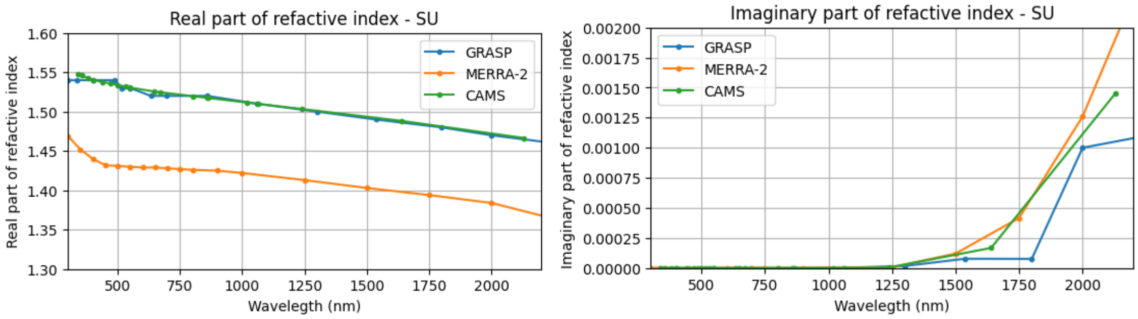

Figure 3.3.1: SU complex refractive index in GRASP chemical component approach, MERRA-2 natural run and CAMS.

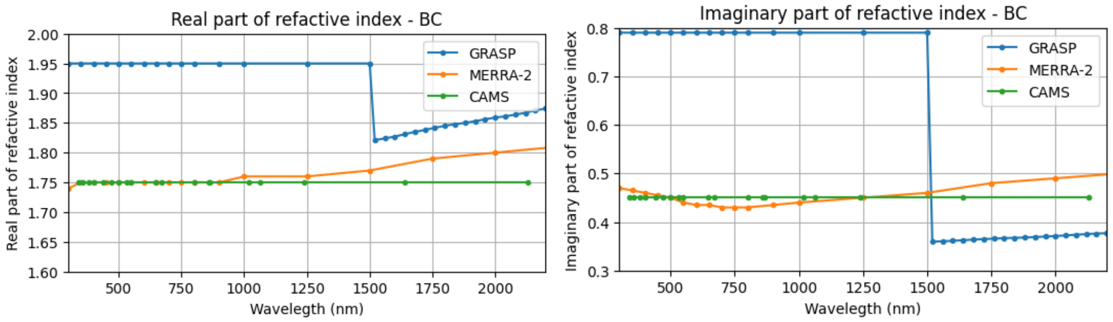

Figure 3.3.2: BC complex refractive index in GRASP chemical component approach, MERRA-2 natural run and CAMS.

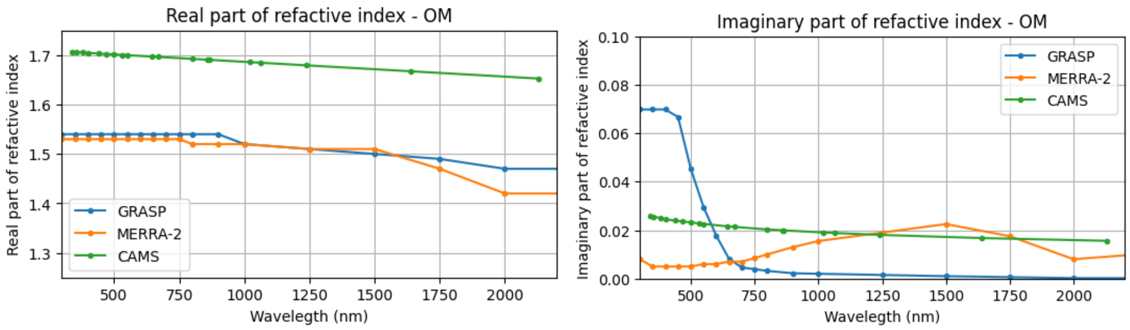

Figure 3.3.3: BrC complex refractive index in GRASP chemical component approach and OM in MERRA-2 natural run and CAMS.

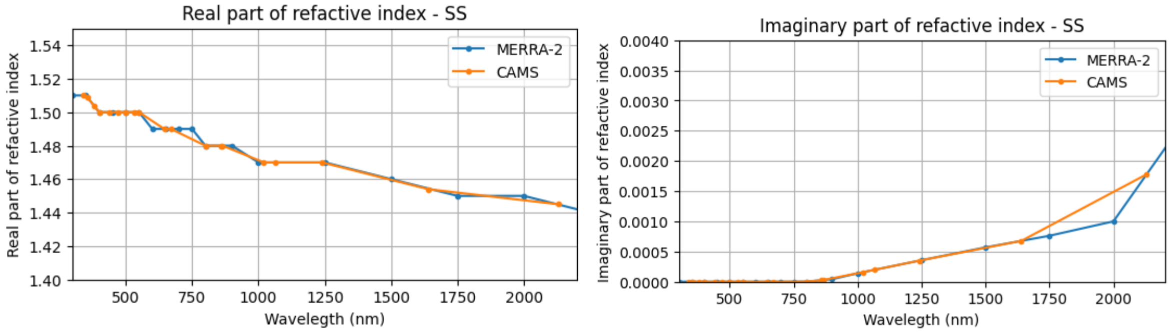

Figure 3.3.4: Sea Salt complex refractive index in GRASP chemical component approach and OM in MERRA-2 natural run and CAMS.

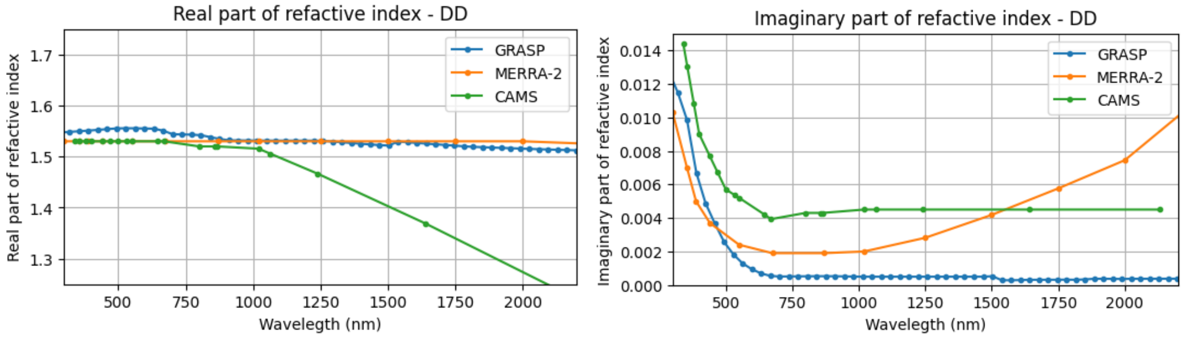

Figure 3.3.5: Dust complex refractive index in GRASP chemical component approach and in MERRA-2 natural run (Shettle and Fenn, 1979) and CAMS (Woodward, 2001).

Table 3.3.1. Refractive indices in MERRA-2, CAMS (cycles 47R1 and 48R1) models used in these studies and GRASP.

Aerosol Species	CAMS	MERRA-2 (GOCART)	GRASP
BC	Hess et al. 1998 (OPAC)	Global Aerosol Data Set (GADS) [Köpke et al. 1997]	Bond and Bergstrom (2006) for Visible, Querry 1987 & Shettle 1979 for TIR
OM	Hess et al. 1998 (OPAC) Brown et al. (2018, ACP)	Global Aerosol Data Set (GADS) [Köpke et al. 1997]	-
BrC	In IFS 48R1 cycle	-	Sun et al., 2007 for vis and NIR; Shettle and Feng 1979 for TIR
SU	Global Aerosol Climatology Project (GACP)	Global Aerosol Data Set (GADS) [Köpke et al. 1997]	Longtine and Shettle 1988
Sea Salt	OPAC	Global Aerosol Data Set (GADS) [Köpke et al. 1997]	-
Dust	Woodward, 2001 (47R1)	GOCART, Shettle and Fenn [1979]	Quartz: Shettle 1987

Aerosol Species	**CAMS**	**MERRA-2 (GOCART)**	**GRASP**
		(Kim et al. 2011) (Buchard et al. 2015).	Iron Oxide: Querry 1987

Complexity of chemical process in atmosphere results in big variability of observed aerosol optical properties and, consequently, in different possibilities of characterization of the refractive index for different aerosol species (Figs. 3.3.1-3.3.5 and Table 3.3.1). The global models like CAMS provides estimation of the global aerosol mass emission. At the same time, remote sensing approaches are sensitive to aerosol optics, in particular, complex refractive index, but not to mass emission. Therefore, harmonization of global models and remote sensing approaches will allow applying much tighter relation between aerosol mass transport, chemistry and optics.

3.3.2 Aerosol species and aerosol modes

CAMS accounts for aerosol as the external mixture of the 5-8 main species (see Table 3.1.1). Aerosol in remote sensing approaches is represented as an external mixture of several aerosol modes (for example, 2 modes in GRASP baseline chemical component approach, Table 3.2.1). Full harmonization between two approaches is possible if each aerosol mode in the remote sensing corresponds to certain aerosol species from CAMS (see for example, Table 3.3.3 for 5 aerosol species from CAMS).

Table 3.3.3 Fully harmonized aerosol models

Aerosol Species in CAMS/MERRA-2	**Remote Sensing Aerosol external mixture mode**						
	1	2	3	4	5	6	7
BC hydrophobic	✓						
BC hydrophilic		✓					
OM hydrophobic			✓				
OM hydrophilic				✓			
SU hydrophilic					✓		
Sea Salt hydrophilic						✓	
Dust							✓

In this case total column volume or number concentration for each mode (Eqs.(3.2.6) and (3.2.7)) can be related to mass mixing ratio of each aerosol species as follows:

$$n_0^{(k)} =< M_{mix}^{(k)}(z)\rho_{air}(z) >/m_{dry}^{(k)}, \tag{3.3.1}$$

$$c_{0v}^{(k)} =< \left(M_{mix}^{(k)}(z)\,\rho_{air}(z)\left[f_{grow}^{(k)}(z)\right]^3\right) >/\rho_{dry}^{(k)}, \tag{3.3.2}$$

where brackets <…> represents the vertical integration. At the same time, adding more modes results in drastic growing of number of the retrieved parameters in remote sensing approaches and, as a result, in rising different kind of problems related to stability of the retrieval and its quality.

3.3.3 Relations to CAMS/MERRA-2 characteristics

As it was described in section 3.2, GRASP baseline chemical component approach includes 2 aerosol modes mixed externally. Each of the modes is represented as internal mixture of different chemical components. The relation between GRASP chemical components and 5 CAMS (or MERRA-2) species is represented in Table 3.3.4.

Table 3.3.4. CAMS aerosol species and GRASP 2 modes

		GRASP chemical components						
Aerosol external mixture		**Fine mode1 (internal mixture)** **3 SD bins**				**Corse mode 2 (internal mixture)** **2 SD bins**		
		BC δ_{BC}	BrC δ_{BrC}	Ammonium Sulphate/ Sea Salt	Quartz δ_{Quartz}^{fine}	Quartz δ_{Quartz}^{coarse}	Ammonium Sulphate/ Sea Salt	FeOx δ_{Iron}
Aerosol Species in CAMS (11 parameters)	BC Hydrophobic	-						
	BC Hydrophilic	-						
	OM Hydrophobic		-					
	OM Hydrophilic	✓	✓	-				
	SU			✓			✓	
	Sea Salt **(3 bins)**			✓			✓	
	Dust **(3 bins)**				✓	✓		✓

The cells with V marks in Table 3.3.4 indicate the existent connections of GRASP baseline chemical component approach with CAMS model. In particular, there are connections between OM hydrophilic in CAMS with internal mixture of BC, BrC Amonium Sulphates/Sea Salt in GRASP: the internal mixture of BC, BrC and soluble in GRASP first mode (Eq. (3.2.8)) is similar to representation of CAMS hydrophilic OM aerosol component (Bozzo et al. 2020). In the second mode dust components (iron-oxide and quartz) are internally mixed with soluble representing Sea Salt (Eq. (3.2.9)).

Volume fractions δ in Eqs. (3.2.8) and (3.2.9) are parameters of the retrieval state vector together with total column concentration for fine $c_{0v}^{(fine)}$ and coarse $c_{0v}^{(coarse)}$ modes of baseline GRASP chemical component approach. They define the total column concentration for each chemical component *k* (Eqs. (3.3.1) and (3.3.2)) and related to it aerosol specie of CAMS model:

$$c_{0v}^{BC} = \delta_{BC}\, c_{0v}^{(fine)},\; c_{0v}^{BrC} = \delta_{BrC} c_{0v}^{(fine)},\; c_{0v}^{SU} = \delta_{SU} c_{0v}^{(fine)}, \qquad (3.3.3)$$

$$c_{0v}^{FeOx} = \delta_{FeOx} c_{0v}^{(coarse)},\; c_{0v}^{Quartz} = \delta_{Quartz} c_{0v}^{(coarse)}. \qquad (3.3.4)$$

Despite already existent cross relations, there are several crucial differences between aerosol models in GRASP baseline chemical component approach and CAMS:

1. Ammonium-sulphate component is always part of internal mixture in GRASP approach whereas SU is the separate specie in CAMS model.
2. Sea Salt component is not well defined in the GRASP baseline approach as separate specie.
3. BC and OM/BrC hydrophobic components are not represented in GRASP as independent species.
4. Dust component in GRASP is represented as an internal mixture of iron-oxide and quartz whereas in CAMS it is presented with a climatological complex refractive index.
5. The complex refractive index of the chemical components and aerosol species can be different (Figs. 3.3.1-3.3.5).
6. Hygroscopic growth in GRASP is represented through retrieval of aerosol size parameters (the concentration of size distribution bins) whereas in CAMS models they depend on Relative Humidity (RH).
7. GRASP operates with column averaged aerosol properties whereas microphysics in CAMS is vertically dependent.

To further harmonize GRASP approach with CAMS model and investigate the most essential information to be accounted for, several feasibility tests were performed and described in the next section.

4 Feasibility studies on harmonisation: based on PARASOL measurements

In this section, we tested the different harmonization schemes based on the POLDER/PARASOL measurements (Sections 4.1-4.5). We process the data (3x3 pixels) over all available AERONET stations for an entire year 2008 and then validate the obtained results with AERONET Level 2 products (Holben et al., 1998; O'Neill et al., 2003; Dubovik and King, 2000). Evaluation of the retrieval performance vs AERONET is performed with statistical characteristics analysis and GCOS-based requirements fulfilment (Global Climate Observing System (GCOS 2016); Popp et al., 2016) (Table 4.1).

Table 4.1. GCOS-based Requirements on aerosol characterization

Characteristics	**Required uncertainty**
AOD	0.04 or 10% (whatever is bigger)
SSA	0.03
AE (443-670)	0.3

4.1 Volume mixture vs Maxwell-Garnett

First of all, the baseline methods using Maxwell-Garnett and Volume-Weighted mixtures are tested and the AERONET validation results are present in Figures 4.1.1 (Maxwell-Garnett) and 4.1.2 (Volume-Weighted). The Chemical Component approach with both Maxwell-Garnett and Volume-Weighted mixing rules for POLDER/PARASOL measurements are documented in Li et al. (2019), (Eqs. (3.2.8) and (3.2.9)). The AERONET validation scheme is the same as described in Chen et al. (2020), and we follow the same criteria to select high quality POLDER retrievals using fitting relative residual (<5% over land and <10% over ocean).

The results for Maxwell-Garnett mixture and the volume mixture are presented in Figs. 4.1.1 and 4.1.2, Tables 4.1.1 and Tables 4.1.2.

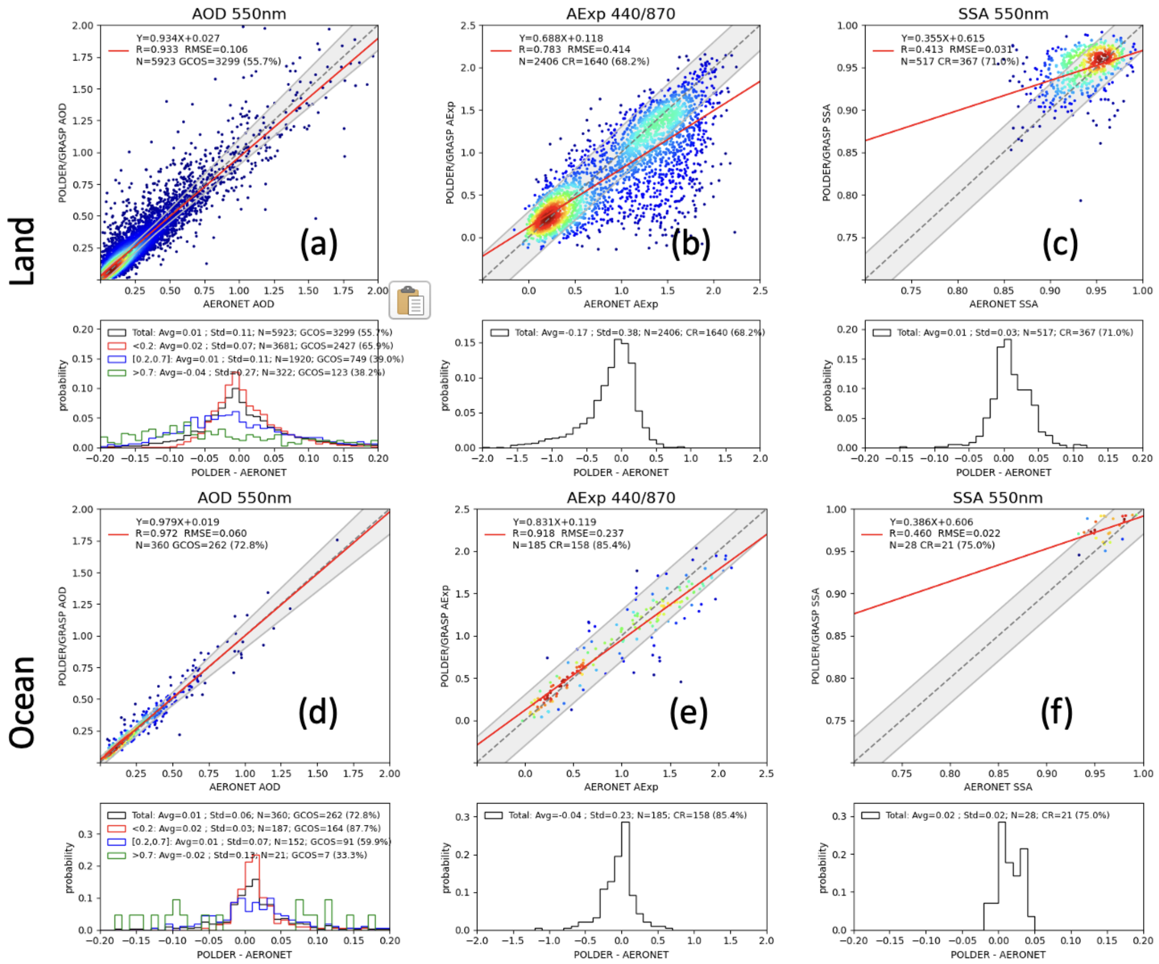

Figure 4.1.1: Validation of POLDER/PARASOL GRASP retrieval with AERONET based on Maxwell-Garnett mixture for an entire year 2008. (a) AOD 550 nm over land; (b) AExp (440/870) over land; (c) SSA 550 nm over land; (d) AOD 550 nm over ocean; (e) AExp (440/870) over ocean; (f) SSA 550 nm over ocean.

Table 4.1.1. Summary of the POLDER/PARASOL GRASP Components retrieval based on Maxwell-Garnett mixture validation statistic metrics with AERONET for AOD (550 nm), AExp (440/870), and SSA (550 nm) over land and ocean.

Land/Ocean	Parameters	R	RMSE	BIAS	GCOS (%)
Land	AOD	0.933	0.106	0.01	55.7
	AExp	0.783	0.414	0.17	68.2
	SSA	0.413	0.031	0.01	71.0
Ocean	AOD	0.972	0.060	0.01	72.8
	AExp	0.918	0.237	-0.04	85.4
	SSA	0.460	0.022	0.02	75.0

One can see that the 2 baseline approaches show good validation results with AERONET. For example, the correlation coefficients for AOD (550 nm) are higher than 0.93 over land and 0.96 over ocean. The fulfilments of GCOS requirements are higher than 50% over land and 60% over ocean. The root-mean-square-error (RMSE) of SSA (550 nm) is smaller than 0.03 both over land and ocean. Even though good agreement is observed in Figures 4.1.1 and

4.1.2, we still see one aspect that has potential to improve that is the overestimation of the retrieved SSA at NIR channels (Figure 4.1.3). Both the obtained SSA (870 nm) from Maxwell-Garnett and Volume-Weighted mixture tend to be slightly higher than AERONET about 0.02, which is possibly related to the pre-described components spectral dependence in this spectrum range and the way how components are mixed together.

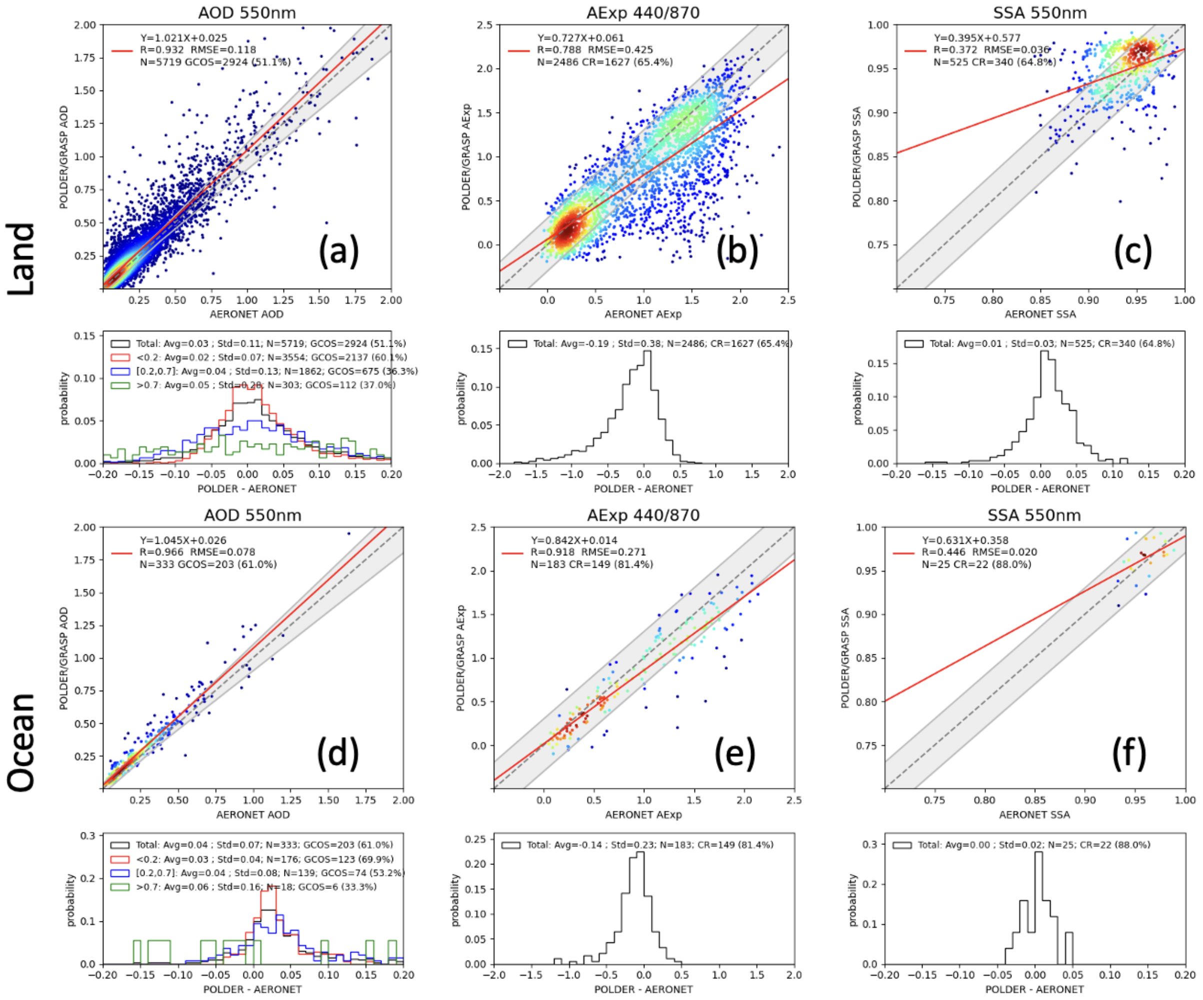

Figure 4.1.2: Validation of POLDER/PARASOL GRASP retrieval with AERONET based on Volume-Weighted mixture for an entire year 2008. (a) AOD 550 nm over land; (b) AExp (440/870) over land; (c) SSA 550 nm over land; (d) AOD 550 nm over ocean (e) AExp (440/870) over ocean; (f) SSA 550 nm over ocean.

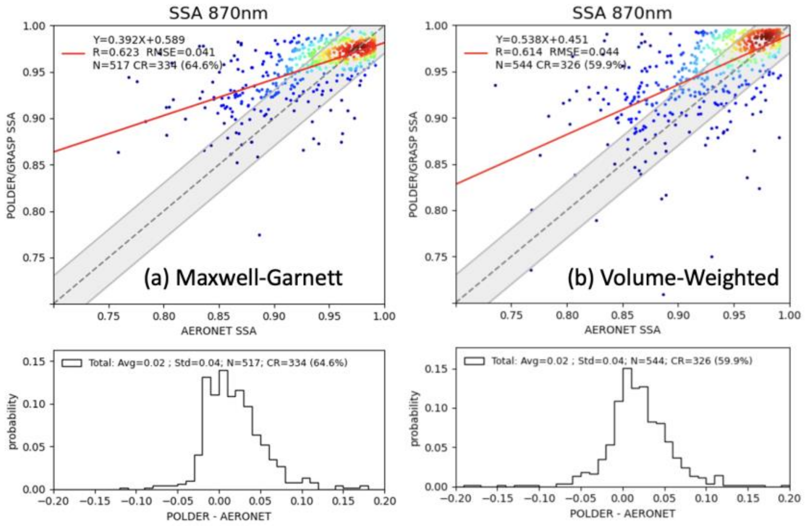

Figure 4.1.3: Validation of POLDER/PARASOL GRASP retrieval of SSA at 870 nm with AERONET inversion product. (a) Maxwell-Garnett mixture; (b) Volume-Weighted mixture.

Table 4.1.2. Summary of the POLDER/PARASOL GRASP Components retrieval based on Volume-Weighted mixture validation statistic metrics with AERONET for AOD (550 nm), AExp (440/870), and SSA (550 nm) over land and ocean.

Land/Ocean	Parameters	R	RMSE	BIAS	GCOS (%)
Land	AOD	0.932	0.118	0.03	51.1
	AExp	0.788	0.452	-0.19	65.4
	SSA	0.372	0.030	0.01	64.8
Ocean	AOD	0.966	0.078	0.04	61.0
	AExp	0.918	0.271	-0.14	81.4
	SSA	0.446	0.020	0.00	88.0

Generally, the results of optical properties obtained from Maxwell-Garnett mixing rule is slightly better than that from Volume-Weighted mixture. However, the Volume-Weighted mixture is close to the treatment in the CAMS model (Section 3), therefore, we will try different harmonization schemes based on the Volume-Weighted mixing rules.

4.2 SU in separate mode

In the original Volume-Weighted mixture, aerosol components are separated into 2 (fine and coarse) modes with fine mode including black carbon, brown carbon, quartz and soluble, and coarse mode including iron oxide, quartz and soluble, where the soluble component is mixed by ammonia sulphate and water (Section 3.2, Table 3.2.1). In this test, we separate sulphate (SU) in an independent fine mode. As a consequence, 2 fine modes + 1 coarse mode are used. The 1st fine mode includes ammonia sulphate (SU) and water, and the 2nd fine mode includes black carbon, brown carbon, quartz and water, and the coarse mode keeps the same as the baseline method. Generally, in this approach, more parameters need to be retrieved, while the separation of SU is similar to CAMS model.

Figure 4.2.1 and Table 4.2.1 show the AERONET validation results of the Volume-Weighted mixture with SU in separate mode. Generally, we observe the quality of AOD and AExp is decreased in terms of AERONET validation metrics with respect to the baseline approach in Figure 4.1.2. For example, the positive bias of AOD becomes non-negligible (~0.06-0.07), and the fulfilment of GCOS requirement is decreased to ~40%. Despite, the R of AOD is still ~0.93 and the SSA at 870 nm slightly improved, the separation of SU in an independent mode does not bring a lot of advantages in the spectral range measurement of POLDER/PARASOL. This can be explained by the fact that adding SU as separate retrieval component increases the number of retrieval parameters and SU contribution can be well described by internal mixture with other chemical components (Eq. (3.2.8)).

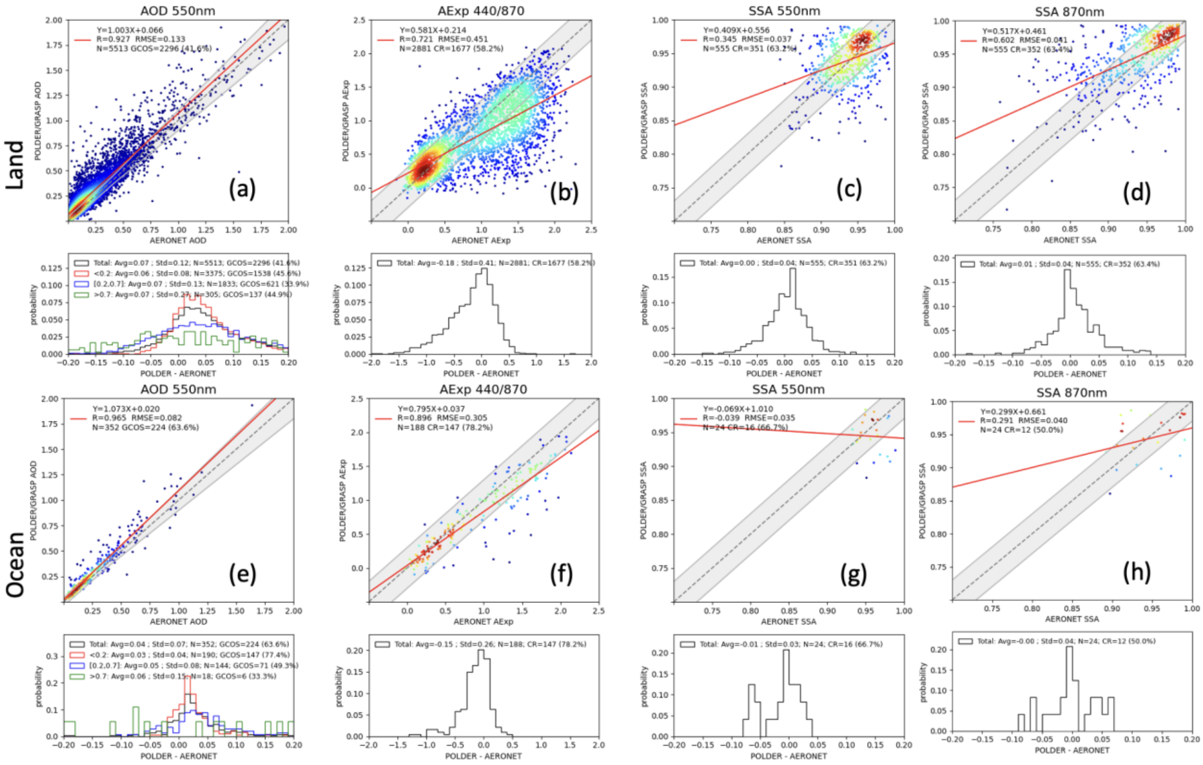

Figure 4.2.1: Validation of POLDER/PARASOL GRASP retrieval with AERONET based on Volume-Weighted mixture (SU in separate mode) for an entire year 2008. (a) AOD 550 nm over land; (b) AExp (440/870) over land; (c) SSA 550 nm over land; (d) SSA 870 nm over land; (e) AOD 550 nm over ocean; (f) AExp (440/870) over ocean; (g) SSA 550 nm over ocean; (h) SSA 870 nm over ocean.

Table 4.2.1. Summary of the POLDER/PARASOL GRASP Components retrieval based on Volume-Weighted mixture (SU in separated mode) validation statistic metrics with AERONET for AOD (550 nm), AExp (440/870), and SSA (550 nm) over land and ocean.

Land/Ocean	Parameters	R	RMSE	BIAS	GCOS (%)
Land	AOD	0.927	0.133	0.06	41.6
	AExp	0.721	0.451	-0.18	58.2
	SSA	0.345	0.037	0.00	63.2
Ocean	AOD	0.965	0.082	0.03	63.6
	AExp	0.896	0.305	-0.15	78.2
	SSA	-0.039	0.035	-0.01	66.7

4.3 Dust and Sea Salt: different species in different modes

In the baseline Volume-Weighted approach, the coarse mode includes iron oxide, quartz and soluble. Iron oxide and quartz are the two components of desert dust, representing absorbing and scattering parts, correspondingly. However, one of the important components is missing, which is Sea Salt. In the CAMS model, the sea salt and dust are the top two contributors of aerosol mass. Therefore, including both sea salt and dust in the coarse modes looks very reasonable. In addition, sea salt particles are hydrophilic and dust particles are mainly hydrophobic. In this test, we include two coarse modes, one hydrophobic coarse mode with iron oxide and quartz, and another hydrophilic coarse mode with sea salt and water. In this test both dust and sea salt are presented as a coarse particles only (by 4th and 5th SD bins Fig.3.2.2 and Table 3.2.2).

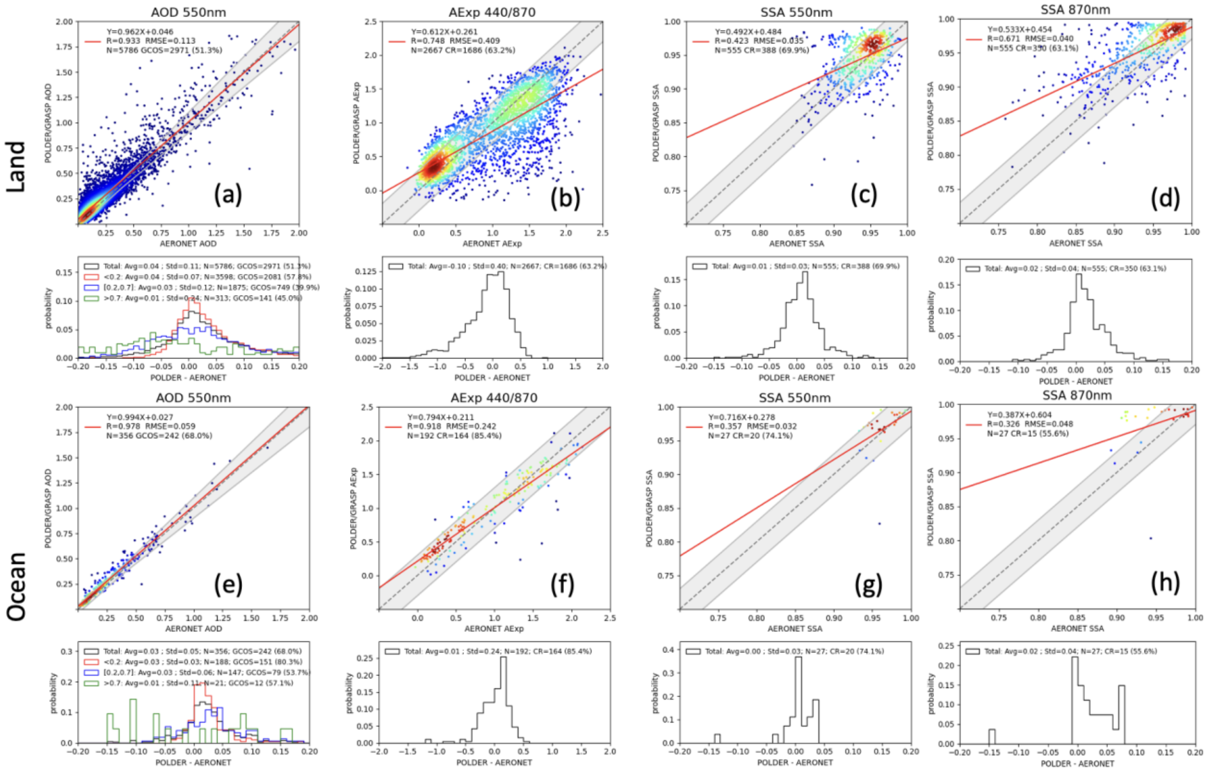

Figure 4.3.1: Validation of POLDER/PARASOL GRASP retrieval with AERONET based on Volume-Weighted mixture (Dust and Sea Salt in separated coarse modes) for an entire year 2008. (a) AOD 550 nm over land; (b) AExp (440/870) over land; (c) SSA 550 nm over land; (d) SSA 870

nm over land; (e) AOD 550 nm over ocean; (f) AExp (440/870) over ocean; (g) SSA 550 nm over ocean; (h) SSA 870 nm over ocean.

Figure 4.3.1 and Table 4.3.1 show the POLDER/PARASOL GRASP retrieval validation with AERONET based on Volume-Weighted mixture (Dust and Sea Salt in separated coarse modes) for an entire year 2008. Basically, the quality of AOD remains comparable with the baseline approach with R ~0.93 and GCOS fraction >50%. Nevertheless, we observe slight improvements of AExp and SSA in terms of AERONET validation, which indicates the benefit from separation of dust and sea salt with the POLDER/PARASOL multi-angular measurements from VIS to NIR.

Table 4.3.1. Summary of the POLDER/PARASOL GRASP Components retrieval based on Volume-Weighted mixture (DD and SS in separated coarse modes) validation statistic metrics with AERONET for AOD (550 nm), AExp (440/870), and SSA (550 nm) over land and ocean.

Land/Ocean	Parameters	R	RMSE	BIAS	GCOS (%)
Land	AOD	0.933	0.113	0.04	51.3
	AExp	0.748	0.409	-0.10	63.2
	SSA	0.423	0.035	0.01	69.9
Ocean	AOD	0.978	0.059	0.03	68.0
	AExp	0.918	0.242	0.01	85.4
	SSA	0.357	0.032	0.00	74.1

Figure 4.3.2 shows the probability density function (PDF) of retrieved complex refractive index and AExp for dust and sea salt modes. The separation of dust and sea salt complex refractive index is clearly seen: the retrieved real part of the complex refractive index for sea salt is almost spectrally independent and imaginary part is very small (non-absorbing particles), while the retrieval for dust shows spectrally dependent real part (~1.55 at 490 nm and ~1.53 at 865 nm), and ~0.001-0.005 for imaginary part. This good distinction between dust and sea salt properties results in improvement of optical properties characterization. Figure 4.3.2 also shows quite essential variability of dust and sea salt complex refractive index, which can be related to different dust mineral composition at different places on Earth and sea salt properties dependence on relative humidity.

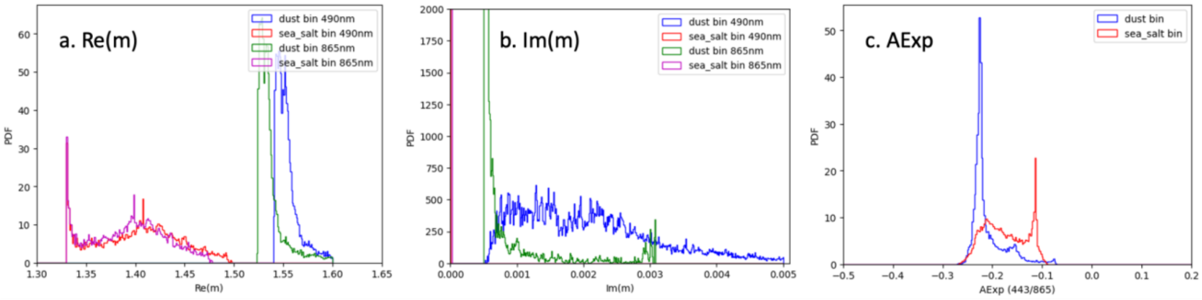

Figure 4.3.2: The probability density function (PDF) of retrieved parameters of dust and sea salt modes: (a) real part of complex refractive index at 490 and 865 nm; (b) imaginary part of complex refractive index at 490 and 865 nm; (c) AExp (443/865).

Figure 4.3.3 shows the spatial distribution of retrieved dust and sea salt complex refractive index at 490 nm and AOD at 443 nm. Qualitatively, we observe reasonable separation of dust and sea salt AOD. For example, the high dust AOD is basically observed over desert and bare soil areas and downwind regions. Over land, the sea salt AOD is generally very low, and it becomes higher at coastal regions and open sea sites, even though it happens to get high sea salt AOD together with high dust AOD, which can be due to transported dust over some ocean AERONET sites.

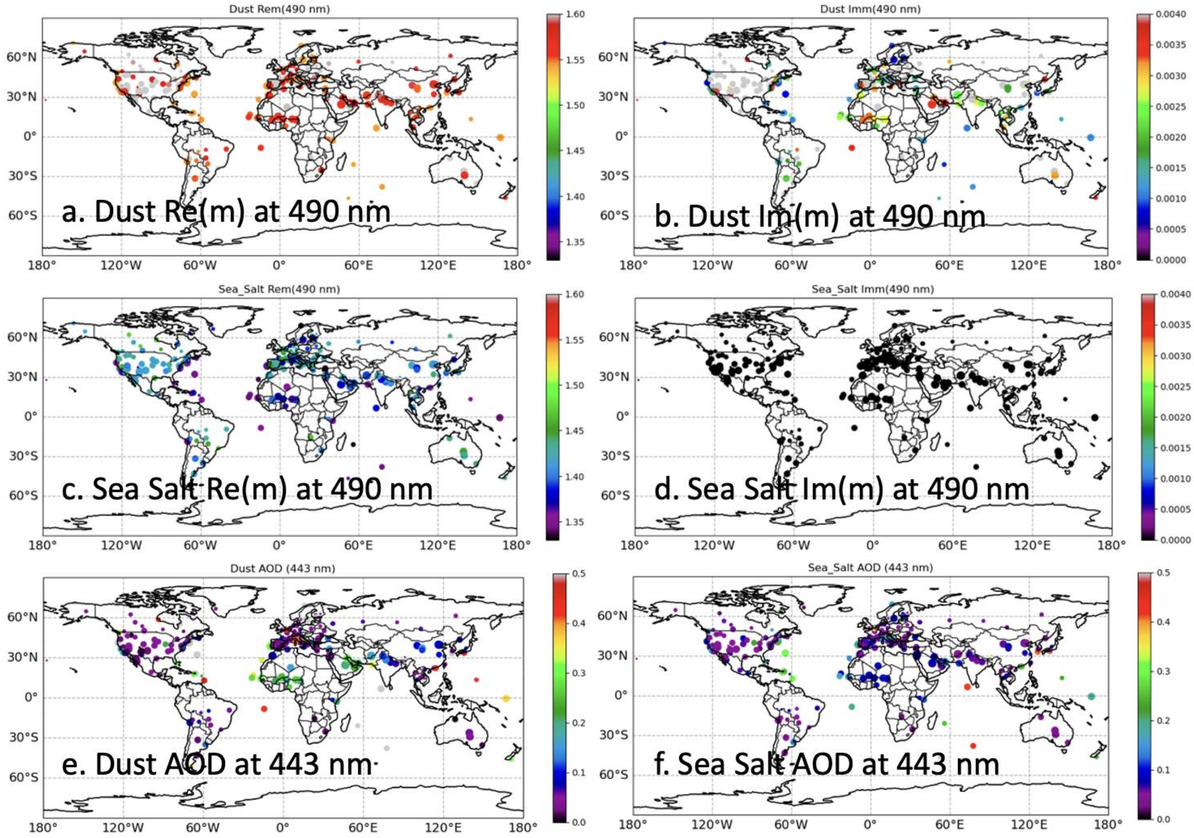

Figure 4.3.3: Spatial distribution of retrieved Dust and Sea Salt complex refractive index at 490 nm and AOD at 443 nm. (a) Dust Re(m) 490 nm; (b) Dust Im(m) 490 nm; (c) Sea Salt Re(m) 490 nm; (d) Sea Salt Im(m) 490 nm; (e) Dust AOD 443 nm; (f) Sea Salt AOD 443 nm.

Overall, the results presented in this section show improvements in the retrieval of the optical characteristics and better discrimination of dust and sea salt aerosol components, when both of them are retrieved as different modes. Such approach allows directly relate retrieved parameters to CAMS characteristics of sea salt and dust. Potentially it can be used to constrain sea salt and dust emission in global transport models.

4.4 Hydrophilic and Hydrophobic BC and BrC

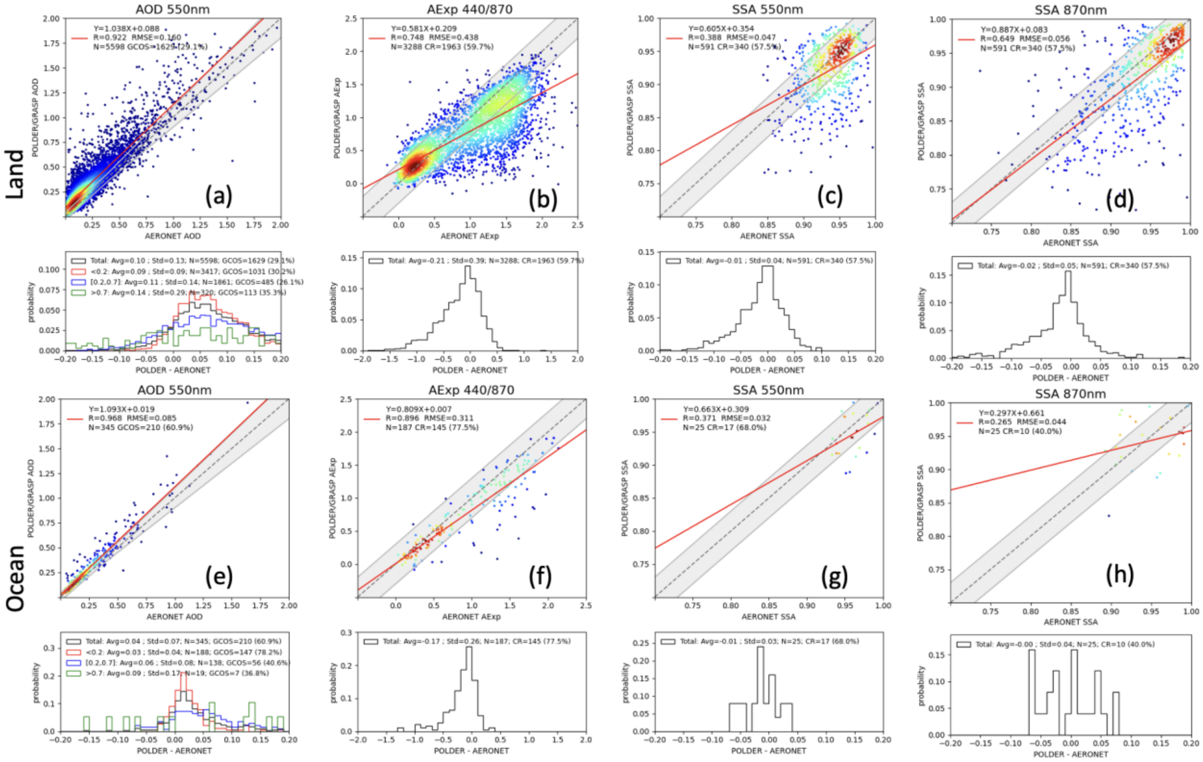

Figure 4.4.1: Validation of POLDER/PARASOL GRASP retrieval with AERONET based on Volume-Weighted mixture (Hydrophilic and hydrophobic BC and BrC in separated fine modes) for an entire year 2008. (a) AOD 550 nm over land; (b) AExp (440/870) over land; (c) SSA 550 nm over land; (d) SSA 870 nm over land; (e) AOD 550 nm over ocean; (f) AExp (440/870) over ocean; (g) SSA 550 nm over ocean; (h) SSA 870 nm over ocean.

Figure 4.4.1 and Table 4.4.1 show the AERONET validation results of the Volume-Weighted mixture with hydrophilic and hydrophobic BC and BrC in separated fine modes. Generally, we observe that the quality of AOD is decreased in terms of AERONET validation metrics with respect to the baseline approach in Figure 4.1.2. For example, the positive bias of AOD becomes non-negligible (~0.09-0.10), and the fulfilment of GCOS requirement is decreased to ~30%. Despite, the R of AOD is still ~0.92 and the SSA at 870 nm slightly improved, the separation of hydrophilic and hydrophobic BC and BrC does not bring a lot of advantages, probably, due to the same reasons as for separate SU mode test: such approach increases the number of retrieved parameters but BC and BrC contribution still can be well described by internal mixture with other chemical components (Eq. (3.2.8)).

Table 4.4.1. Summary of the POLDER/PARASOL GRASP retrieval with AERONET based on Volume-Weighted mixture (Hydrophilic and hydrophobic BC and BrC in separated fine modes) validation statistic metrics with AERONET for AOD (550 nm), AExp (440/870), and SSA (550 nm) over land and ocean.

Land/Ocean	Parameters	R	RMSE	BIAS	GCOS (%)
Land	AOD	0.922	0.160	0.09	29.1
	AExp	0.748	0.438	-0.21	59.7
	SSA	0.388	0.047	-0.01	57.5
Ocean	AOD	0.968	0.085	0.03	60.9

Land/Ocean	Parameters	R	RMSE	BIAS	GCOS (%)
	AExp	0.896	0.311	-0.17	77.5
	SSA	0.371	0.032	-0.01	68.0

4.5 Refractive index harmonization: the use of CAMS BC

As presented in Figures 3.3.2 and 3.3.3, the refractive index for BC and OC used in GRASP/Component approach has essential differences with CAMS. Generally, GRASP/Component uses the BC CRI from Querry, 1987 as well as Bond and Bergstrom (2006), while CAMS and MERRA-2 refractive indices for this test correspond to the OPAC database with some modifications (Hess et al., 1998) (Table 3.3.1). In order to test how the selection of BC and OC refractive index will affect the retrievals, we use the baseline GRASP/Component approach with Maxwell-Garnett mixture and replace original GRASP BC and BrC refractive index with CAMS/MERRA-2 BC and MERRA-2 OC and applied on the POLDER/PARASOL measurements. In addition, we tested another option: GRASP refractive index was used for BC and MERRA-2 one for OC refractive index. In this study MERRA-2 refractive indices were selected due to similarity of BrC refractive indices used in GRASP and ease of harmonisation, that doesn’t reach values of real part of refractive index that are not included in the GRASP single scattering kernels (n=1.7, see Fig.3.3.3), and, at the same time, significant similarity of the BC values between MERRA-2 and CAMS (see Fig. 3.3.2), allowing to draw similar conclusions for the case of BC refractive index sensitivity.

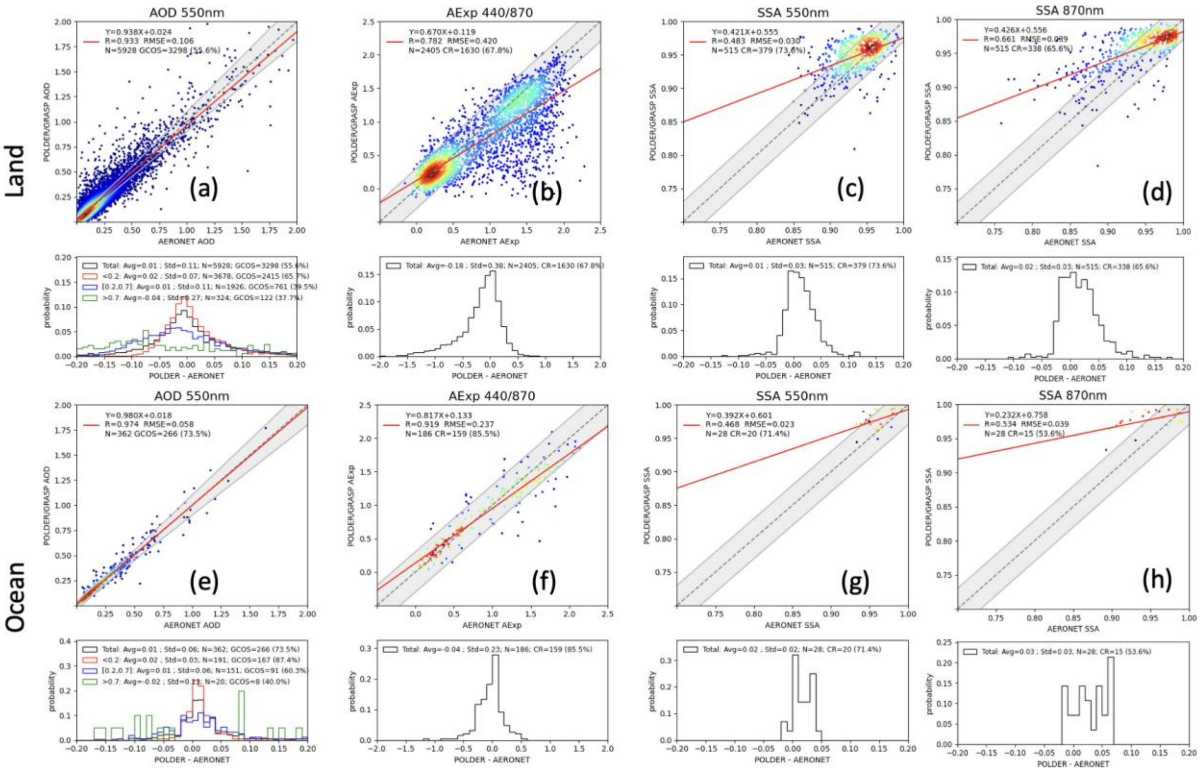

Figure 4.5.1: Validation of POLDER/PARASOL GRASP retrieval with AERONET based on Maxwell-Garnett mixture (update with MERRA-2 BC and OC refractive index) for an entire year 2008. (a) AOD 550 nm over land; (b) AExp (440/870) over land; (c) SSA 550 nm over land; (d) SSA 870 nm over land; (e) AOD 550 nm over ocean; (f) AExp (440/870) over ocean; (g) SSA 550 nm over ocean; (h) SSA 870 nm over ocean.

As shown in Figure 4.5.1 and Table 4.5.1, in comparison with the GRASP/Components Maxwell-Garnett baseline results in Figure 4.1.1, the change of different BC and OC complex refractive index almost has only minor effects on the retrieval of aerosol optical and microphysical properties. It implies that we obtain different volume / mass of aerosol components based on different assumptions on refractive index. Therefore, we further look at the retrieval of aerosol volume fractions, particularly for BC, since the CAMS/MERRA-2 BC refractive index is 1.75-0.44i at 550 nm while GRASP baseline approach uses 1.95-0.79i. Figure 4.5.2 shows the time series of retrieved BC volume fraction over 3 typical sites (Mongu, Kanpur and Ilorin) based on GRASP/Component Maxwell-Garnett mixture approach: (i) GRASP BCOC - baseline approach; (ii) MERRA-2 BCOC - updated with MERRA-2 BC and OC refractive index; (iii) MERRA-2 OC - updated with MERRA-2 OC and GRASP BC refractive index is used. Generally, we observe higher BC volume fraction associated with less absorption assumption of it (1.75-0.44i). Overall, the difference of obtained BC concentration between m=1.75-0.44i and m=1.95-0.79i can be about a factor of 1.5-2.

Table 4.5.1. Summary of the POLDER/PARASOL GRASP retrieval with AERONET based on Maxwell-Garnett mixture (update with CAMS/MERRA-2 BC and OC refractive index) validation statistic metrics with AERONET for AOD (550 nm), AExp (440/870), and SSA (550 nm) over land and ocean.

Land/Ocean	Parameters	R	RMSE	BIAS	GCOS (%)
Land	AOD	0.933	0.106	0.01	55.6
	AExp	0.782	0.420	-0.18	67.8
	SSA	0.483	0.030	0.01	73.6
Ocean	AOD	0.974	0.058	0.01	73.3
	AExp	0.919	0.237	-0.04	85.5
	SSA	0.468	0.023	0.02	71.4

Such difference in the retrieved volume fraction of different chemical components results in essential difference of volume and mass concentration (Fig.4.5.3). In particular, with m=1.75-0.44i for BC the volume concentration is about 1.75-1.8 higher than for BC m=1.95-0.79i. For mass concentration the ratio is about 1.8-1.9.

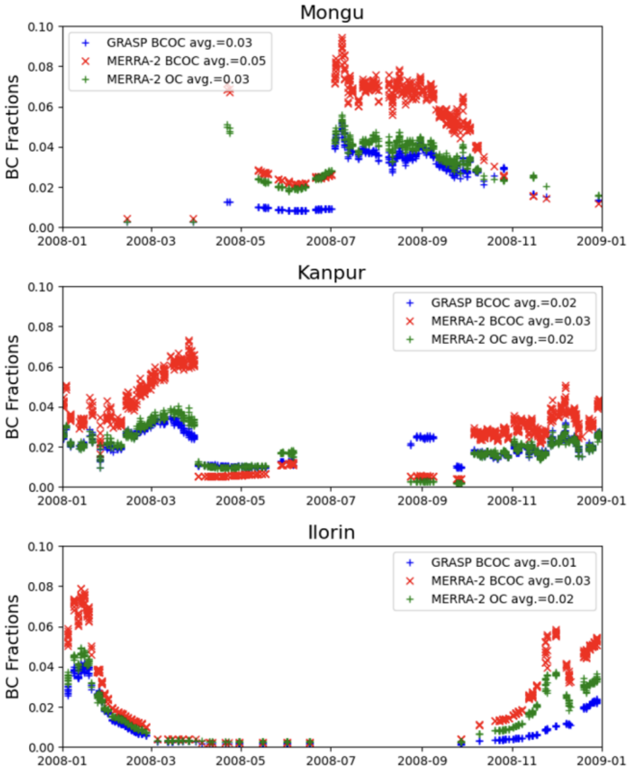

Figure 4.5.2: Time series of retrieved BC volume fractions over 3 typical sites (Mongu, Kanpur and Ilorin) based on GRASP/Component Maxwell-Garnett mixture approach: (i) GRASP BCOC - baseline approach; (ii) MERRA-2 BCOC - updated with MERRA-2 BC and OC refractive index; (iii) MERRA-2 OC - updated with MERRA-2 OC and keep GRASP BC.

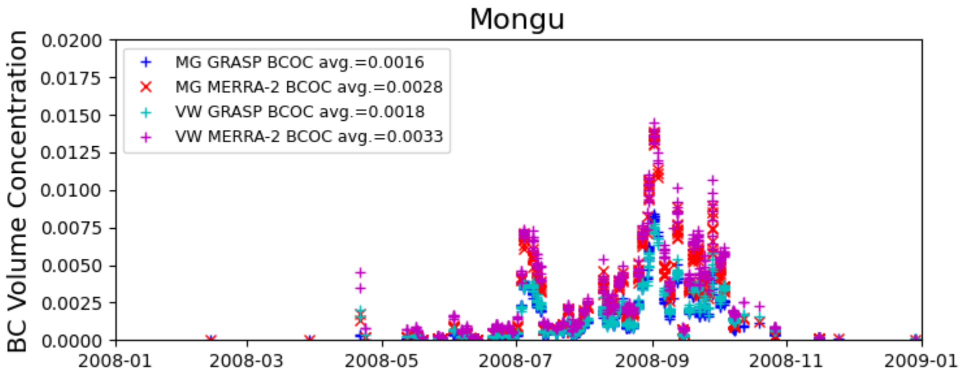

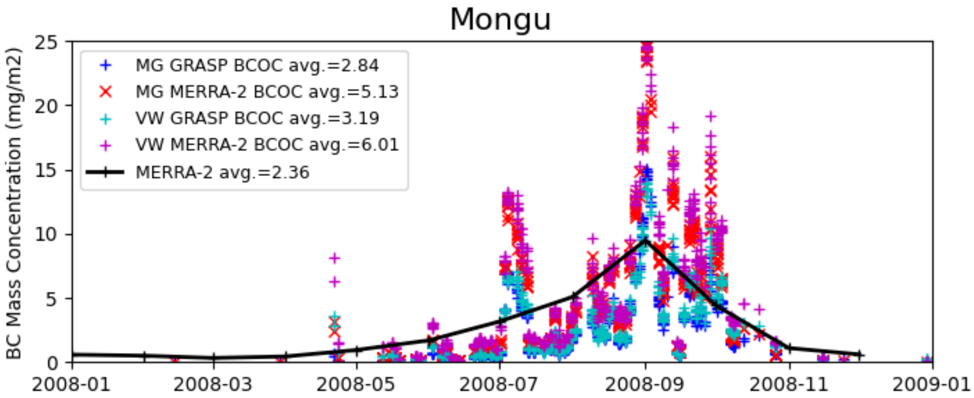

Figure 4.5.3: Time series of retrieved BC volume and concentrations over Mongu: (i) GRASP BCOC - baseline approach; (ii) MERRA-2 BCOC - updated with CAMS/MERRA-2 BC and MERRA-2OC refractive index; (iii) VW GRASP BCOC similar to (i) but for volume weighted mixture; (iv) VW MERRA-2 BCOC similar to (ii) but for volume weighted mixture.

5 Summary on harmonization of aerosol models

Feasibility studies on retrieval of CAMS/MERRA-2 parameters from remote sensing demonstrated that harmonization of remote sensing retrieval approaches with global transport models is relatively straightforward but several questions should be clarified:

1. The most optimal set of independent aerosol modes which on one hand satisfies the need of remote sensing and on another hand allows direct retrieval of essential parameters of global models.
2. Harmonized spectral dependence between aerosol components of remote sensing and aerosol species on global models.
3. More physical accounting for hygroscopic growth with relative humidity in remote sensing retrieval
4. Possibility of accounting more complex vertical structure of atmosphere in remote sensing approaches, for example, different vertical distribution for different aerosol modes in remote sensing.

The answer on these and other similar questions depends on remote sensing measurements which are used as input for retrieval. These feasibility studies were focused on multi-angular, multi-spectral polarimetric measurements, which provide comparably big information content about aerosol. In particular, different GRASP retrieval approaches were tested on real PARASOL observations. It was shown that direct implementation of CAMS or MERRA-2 aerosol modelling approach for retrieval of multi-angular polarimetric measurements may not be the best option. The proper balance between model complexity and optimal number of the retrieved parameters should be accounted for. These results are summarised in Table 5.1, where several feasibility tests were focused on the harmonization. In particular,

i. Separation of SU, hydrophobic BC and OM/BrC into independent aerosol mode, similarly to the CAMS and MERRA-2 models, does not show conclusive improvements of retrieval: AOD and AExp quality decreased, but SSA retrieval was improved. This may be due to the fact that such approaches increase the number of retrieved parameters but SU, BC and BrC contribution still can be well described by internal mixture with other chemical components already presented in one of the aerosol modes in GRASP chemical component approach.
ii. Putting Sea Salt and Dust aerosol components in separate modes allowed, on one hand, achieve better harmonization with CAMS and MERRA-2 models and, on another hand, improve the results of SSA retrieval. Such effects can be explained by very different microphysical and hygroscopic properties of Sea Salt and Dust, which introduced additional sensitivity to the way of their description in remote sensing retrieval.
iii. Harmonization of the complex refractive index from GRASP chemical component approach with CAMS and MERRA-2 models showed similar performance of the retrieved optical properties on real PARASOL measurements. Such limited sensitivity to the spectral dependence of the chemical components in real measurements can be explained by compensation effect provided by the internal mixture with water component: for example, quite similar effective refractive index for internally mixed BC and water components can be obtained either by smaller amount of the more absorbing BC component and bigger amount of water or by bigger amount of less absorbing BC and less amount of water.

Table 5.1. Feasibility tests summary

	Feasibility tests	Performance in AOD	Performance in SSA	Performance in AE
1	Volume mixture	Same quality	Same quality	Same quality
2	SU in separate mode	Decreased	Improved	Decreased
3	Sea Salt and Dust in separates modes	Same quality	Improved	Improved
4	Hydrophobic BC and BrC in the separate modes	Decreased	Improved	Decreased
5	Adjustment of the complex refractive index of aerosol chemical components	Same quality	Same quality	Same quality

Several questions require further detailed investigation to harmonize aerosol models from remote sensing and global models. In particular, the following studies are still have to be carried out:

- Physically based accounting for aerosol hygroscopic growth with relative humidity in remote sensing approaches. Such will allow reduce the number of parameters in remote sing retrieval and tight relations between aerosol parameters derived from remote sensing and global models.
- Different assumption on aerosol size distribution in remote sensing and CAMS/MERRA-2 models
- Accounting for aerosol microphysics vertical properties dependence in remote sensing approaches. This will be especially useful when additional information about atmosphere vertical structure is available, for example, from synergy of polarimetric and LIDAR measurements.
- Accounting for non-sphericity and particle inhomogeneity in CAMS and MERRA-2 models. Aerosol non-sphericity may affect the atmosphere radiance calculations and thus the estimation of energy balance.
- Redundancy of external mixture of aerosol components in remote sensing when internal one is taken into account. Feasibility tests did not show essential improvements of the retrieval when both external and internal mixture of the same chemical component is accounted for (for example, internal and external mixture of BC, OC/BrC, SU). The studies were performed over AERONET stations which may not capture some very specific aerosol mixtures. Extending these studies to global or regional scale may be helpful in these regards.
- The spectral refractive index of the main aerosol species (and especially BC and Dust) may strongly affect the value of volume and mass concentration derived from remote sensing retrieval. Further harmonization between remote sensing and CAMS model is necessary to provide correct aerosol mass estimation in atmosphere.

6 References

Bond, T. C. and Bergstrom, R. W.: Light Absorption by Carbonaceous Particles: An Investigative Review, Aerosol Sci. Tech., 40, 27–67, https://doi.org/10.1080/02786820500421521, 2006.

Bozzo, A., A. Benedetti, J. Flemming, Z. Kipling, and S. Rémy. An aerosol climatology for global models based on the tropospheric aerosol scheme in the Integrated Forecasting System of ECMWF. Geosci. Model Dev., 13, 1007–1034, 2020. https://doi.org/10.5194/gmd-13-1007-2020.

Castellanos, P., and da Silva, A., 2019: A neural network correction to the scalar approximation in radiative transfer, J. Atmos. Oceanic Tech., 36, 819-832, https://doi.org/10.1175/JTECH-D-18-0003.1

Chen, C., O. Dubovik, D. Fuertes, P. Litvinov, T. Lapyonok, A. Lopatin, F. Ducos, Y. Derimian, M. Herman, D. Tanré, L. A. Remer, A. Lyapustin, A. M. Sayer, R. C. Levy, C. Hsu, J. Descloitres, L. Li, B. Torres, Y. Karol, M. Herrera, M. Herreras, M. Aspetsberger, M. Wanzenboeck, L. Bindreiter, D. Marth, A. Hangler, and C. Federspiel, Validation of GRASP algorithm product from POLDER/PARASOL data and assessment of multi-angular polarimetry potential for aerosol monitoring, Earth System Science Data, 12, 3573–3620, https://doi.org/10.5194/essd-12-3573-2020, 2020.

Chin M., Ginoux P., Kinne S., Torres O., Holben B., Duncan B., Martin R., Logan J., Higurashi A., and Nakajima T. Tropospheric Aerosol Optical Thickness from the GOCART Model and Comparisons with Satellite and Sun Photometer Measurements. J. Atm. Sci., 59, 2002

Dubovik, O., & King, M. D. (2000). A flexible inversion algorithm for retrieval of aerosol optical properties from Sun and sky radiance measurements. Journal of Geophysical Research: Atmospheres, 105(D16), 20673–20696. https://doi.org/10.1029/2000JD900282

Flemming, J., Benedetti, A., Inness, A., Engelen, R. J., Jones, L., Huijnen, V., Remy, S., Parrington, M., Suttie, M., Bozzo, A., Peuch, V.-H., Akritidis, D., and Katragkou, E.: The CAMS interim Reanalysis of Carbon Monoxide, Ozone and Aerosol for 2003–2015, Atmos. Chem. Phys., 17, 1945–1983, https://doi.org/10.5194/acp-17-1945-2017, 2017.

Flemming, J., Huijnen, V., Arteta, J., Bechtold, P., Beljaars, A., Blechschmidt, A.-M., Diamantakis, M., Engelen, R. J., Gaudel, A., Inness, A., Jones, L., Josse, B., Katragkou, E., Marecal, V., Peuch, V.-H., Richter, A., Schultz, M. G., Stein, O., and Tsikerdekis, A.: Tropospheric chemistry in the Integrated Fore- casting System of ECMWF, Geosci. Model Dev., 8, 975–1003, https://doi.org/10.5194/gmd-8-975-2015, 2015.

GCOS, 2016: The Global Observing System for Climate: Implementation Needs (GCOS200).

Granier, C., Bessagnet, B., Bond, T., D'angiola, A., van der Gon, H. D., Frost, G. J., Heil, A., Kaiser, J. W., Kinne, S., Klimont, Z., Kloster, S., Lamarque, J.-F., Liousse, C., Masui, T., Meleux, F., Mieville, A., Ohara, T., Raut, J.-C., Riahi, K., Schultz, M. G., Smith, S. J., Thompson, A., van Aardenne, J., van der Werf, G. R., and van Vuuren, D. P.: Evolution of anthropogenic and biomass burning emissions of air pollutants at global and re- gional scales during the 1980–2010 period, Clim. Change, 109, 163, https://doi.org/10.1007/s10584-011-0154-1, 2011.

Hess, M., Koepke, P., and Schult, I.: Optical Properties of Aerosols and Clouds: The Software Package OPAC, B. Am. Meteorol. Soc., 79, 831–844, https://doi.org/10.1175/1520-0477(1998)079<0831:OPOAAC>2.0.CO;2, 1998.

Kaiser, J. W., Heil, A., Andreae, M. O., Benedetti, A., Chubarova, N., Jones, L., Morcrette, J.-J., Razinger, M., Schultz, M. G., Suttie, M., and van der Werf, G. R.: Biomass burning emis- sions estimated with a global fire assimilation system based on observed fire radiative power, Biogeosciences, 9, 527–554, https://doi.org/10.5194/bg-9-527-2012, 2012.

Li., L., O. Dubovik, Y. Derimian, G. L. Schuster, T. Lapyonok, P. Litvinov, F. Ducos, D. Fuertes, C. Chen, Z. Li, A. Lopatin, B. Torres and H. Che, “Retrieval of aerosol components directly from satellite and ground-based measurements”, Atmos. Chem. Phys. 19, 13409–13443, https://doi.org/10.5194/acp-19-13409-2019, 2019.

Monahan, E. C., Spiel, D. C., and Davidson, K. L.: A model of marine aerosol generation via whitecaps and wave disruption, in: Oceanic Whitecaps, edited by: Monahan, E. C. and Mac Niocaill, G., D. Reidel, Norwell, Massachusetts, 167–174, 1986

Holben, B. N., Eck, T. F., Slutsker, I., Tanré, D., Buis, J. P., Setzer, A., et al. (1998). AERONET—A Federated Instrument Network and Data Archive for Aerosol Characterization. Remote Sensing of Environment, 66(1), 1–16. https://doi.org/10.1016/S0034-4257(98)00031-5

O’Neill, N. T., Eck, T. F., Smirnov, A., Holben, B. N., & Thulasiraman, S. (2003). Spectral discrimination of coarse and fine mode optical depth. Journal of Geophysical Research D: Atmospheres, 108(17). https://doi.org/10.1029/2002jd002975

Popp, T., de Leeuw, G., Bingen, C., Brühl, C., Capelle, V., Chedin, A., et al. (2016). Development, Production and Evaluation of Aerosol Climate Data Records from European Satellite Observations (Aerosol_cci). *Remote Sensing*, *8*(5), 421. https://doi.org/10.3390/rs8050421

Randles, C., da Silva, A., Buchard, V., Colarco, P. R., Darmenov, V., Govindaraju, R., Smirnov, A., Holben, B., Ferrare, R., Hair, J., Shinozuka, Y., and Flynn, C., J., 2017: The MERRA-2 aerosol reanalysis, 1980, onward: Part I: System description and data assimilation evaluation, J. Climate, 30, 6823-6250, https://doi.org/10.1175/JCLI-D-16-0609.1

Rémy, S., Kipling, Z., Huijnen, V., Flemming, J., Nabat, P., Michou, M., Ades, M., Engelen, R., and Peuch, V.-H. (2022). Description and evaluation of the tropospheric aerosol scheme in the Integrated Forecasting System (IFS-AER, cycle 47R1) of ECMWF. Geosci. Model Dev., 15, 4881–4912.

Document History

Version	Author(s)	Date	Changes
0.1	Pavel Litvinov, Oleg Dubovik, Cheng Chen, Milagros Herrera, Christian Matar, Marcos Herreras, Anton Lopatin	13/12/2023	Initial version
1.0	As above	Jan 2024	Updates after internal review

Internal Review History

Internal Reviewers	Date	Comments
(ECMWF) and Yana Karol (GRASP)	Dec 2023 and Jan 2024	